Proceedings Eighth Workshop Geothermal Reservoir Engineering
Stanford University, Stanford, California, December 1982
SGP-TR-60

HEAT EXTRACTION MODELING OF THE STANFORD HYDROTHERMAL RESERVOIR MODEL

A. Hunsbedt, S. T. Lam, and P. Kruger
Stanford Geothermal Program
Stanford University
and
K. Pruess
Earth Sciences Division
Lawrence Berkeley Laboratory

INTRODUCTION

Long-term commercial development of geothermal resources for electric power production will depend on significant heat extraction from hydrothermal reservoir rock as well as production of hot water. The study of heat extraction in the Stanford Geothermal Program has concentrated on developing a useful model for estimating the potential for heat extraction from fractured hydrothermal reservoirs. The project encompasses a physical model for data acquisition and mathematical models for interpretation of the results.

The physical model consists of a pressure vessel containing a rock matrix simulating a fractured hydrothermal reservoir. Early rock loadings consisted of irregular shape rock fragments of various sizes (Hunsbedt, Kruger, and London 1977, 1978) to develop the production characteristics and a one-dimensional cold-water sweep model. The current rock loading consists of granite rock blocks having regular shape, closer packing of the rocks, and a larger average rock size. Flow conditions in this rock configuration can be varied to obtain a large range of rock-to-water temperature differences. These conditions were designed to test the equivalent rock radius approach used in the one-dimensional sweep model. The experimental data are also used to assist in the development of more sophisticated numerical models of thermal production from hydrothermal reservoirs.

A major parameter in the one-dimensional sweep model is the effective number of heat transfer units, N_{tu}, which indicates the extent of heat extraction from the reservoir rock. Results of the first experiment with the current rock loading at $N_{tu} = 7$ were presented by Swenson and Hunsbedt (1981). Subsequently, two additional heat extraction experiments were performed. One of these was at a higher flowrate to reduce the N_{tu} parameter to 2 and the other was at a lower flowrate to yield a N_{tu} parameter of 15. A fourth experiment was performed to calibrate the heat loss calculation in the mathematical model without fluid injection and production.

This paper summarizes the experimental results and the current mathematical modeling efforts using the one-dimensional sweep model and the LBL numerical reservoir simulator.

HEAT EXTRACTION EXPERIMENTS

The SGP physical model has been described in several reports, e.g., Hunsbedt, Kruger, and London (1977, 1978). The reservoir is a 1.52 m (5 ft) high by 0.61 m (2 ft) diameter insulated pressure vessel. The rock matrix used in these experiments consists of 30 granite rock blocks of 0.19 x 0.19 m (7.5 x 7.5 inches) rectangular cross section and 24 triangular blocks as shown in Figure 1. The blocks are 0.26 m (10.4 inches) high. The average porosity of the matrix is 17.5 percent.

Vertical channels between blocks are spaced at 0.0064 m (0.25 inch) and horizontal channels between layers are spaced at 0.0043 m (0.17 inch). Significant vertical flow can also occur in the relatively large edge channels between the outer rock blocks and the pressure vessel.

Cold water is injected at the bottom of the vessel by a high pressure pump through a flow distribution baffle at the inlet to the rock matrix. System pressure is maintained above saturation by a flow control valve downstream of the vessel outlet. Most of the system pressure drop is in this valve while the rock matrix has essentially infinite permeability.

The water temperature is measured at the several locations shown in Figure 1: the inlet to the vessel, the I-plane just below the baffle, the B-plane half-way up the first rock layer, the M-plane half-way up the third rock layer, the T-plane near the top of the rock matrix, and the vessel outlet. Temperatures are also measured at the center of four rock blocks. The bottom central rock, to be used to examine effects of repeated thermal stressing on heat transfer properties, has two additional thermocouples.

For the three N_{tu} parameter experiments, the rock-water-vessel system was heated to the uniform initial temperatures indicted in Table 1 by electric strap heaters outside the vessel. Heat extraction was initiated by starting the injection pump and opening the flow control valve. The injection rate was constant during the experiments. Data for

the reservoir conditions and parameter values for these experiments are summarized in Table 1.

For the heat loss calibration experiment, the system was heated to a uniform temperature of about 242°C. The vessel isolation valves in the inlet and outlet lines of the vessel were closed during this experiment. Temperature and pressure data were recorded as the system cooled down as a result of heat loss through the vessel insulation and through metal objects protruding from the vessel.

EXPERIMENTAL RESULTS

Measured water and rock temperature data for the three heat extraction experiments are given in Figures 2 to 4. The locations of the measurement planes are indicated in Figure 1. The temperature of the water entering from the distribution baffle below the rock matrix, indicated by thermocouples IW1 and IW2, decreases approximately exponentially from temperature levels near the initial matrix temperature to the injection water temperature indicated by thermocouple 109. The inlet water temperature appears to be relatively uniform in all experiments except for experiment 5-2 (Figure 3). The maximum temperature difference between water entering the rock matrix at the bottom is about 38°C (100°F). This large nonuniformity in entering water temperature is probably caused by the higher heating rate from the steel vessel lower head and flanges when cooled more rapidly by the higher water flowrate.

The water temperature distribution in the other three measurement planes were observed to be quite uniform. The maximum temperature difference or range of water temperature data was usually less than 5°C (9°F). The water temperatures given in the figures for the B-, M-, and T-planes are the averages of all thermocouples in each plane. Since the uncertainty interval of the temperature measurements is estimated to be 3°C (5°F), it is concluded that water temperatures in the various flow channels appears to be virtually uniform, indicating good cross mixing between flow channels.

The effect of water flowrate on rock-to-water temperature differences is also indicated in Figures 2 through 4. The maximum temperature difference developed was about 150°C (270°F) for experiment 5-2 with the highest water flowrate to 28°C (50°F) for experiment 5-3 with the lowest flowrate. The maximum temperature difference occurred in the bottom plane that experiences the highest cooldown.

Although high rock-to-water temperature differences result in higher rates of heat extraction from the rock, insufficient heating of the water may result in premature drop in produced water temperatures for high water flowrates. In that case much of the energy stored in the rock is not utilized. The premature drop in produced water temperature as a function of water flowrate is not clearly illustrated in the experimental results because of the effects of total heat losses from the vessel which are much larger for experiment 5-3, lasting for about 10.5 hr as compared to experiment 5-2, lasting only 1.5 hr. The steady drop in produced water temperature in Figure 4 is caused by greater vessel insulation heat losses to the environment because of the longer time period involved.

Mathematical modeling of the experimental system requires accurate data of this heat loss term as a function of production time. The low flowrate experiments last for longer time periods, and the heat loss term becomes a more important factor in the heat balance equation relative to the rock heat extraction term. Data from the calibration cooldown experiments are expected to reduce the uncertainty in the net heat extraction from the rock matrix. Average water and rock temperatures inside the vessel for the calibration experiment are given in Figure 5. The data are compared to the average water temperature data obtained from an earlier experiment. The agreement between these two experiments is very good, and the difference is probably caused by different volumetric heat capacitances of the two test systems.

Table 1
EXPERIMENTAL DATA AND PARAMETERS

	Heat Extraction Experiment		
	5-1	5-2	5-3
Average Reservoir Pressure (MPa)	3.8	3.8	3.6
Initial Reservoir Temperature (°C)	239	220	220
Final Water Temperature at Top (°C)	156	125	141
Final Water Temperature at Bottom (°C)	19	20	28
Injection Water Temperature (°C)	15	15.6	18.3
Injected Water Mass (kg)	340	341	330
Water Injection Rate (kg/hr)	68	227	31.4
Production Time (hr)	5	1.5	10.5

NUMERICAL MODELING

The results of these heat extraction experiments are being examined with a distributed parameter model (Pruess and Schroeder, 1980). All important processes involved in the thermal sweep model are represented: (1) upflow of water through the void spaces in the vessel, (2) heat conduction in the rocks, (3) heat transfer from the rock blocks to the water, (4) heat transfer between water and the walls of the vessel, (5) heat conduction in the walls, and (6) heat transfer between the walls and the surroundings.

The basic computational mesh is shown in Figure 6, which also indicates the major subdomains to be treated in the modeling effort. The main portion of the mesh is a two-dimensional r-z system, with additional irregularly shaped grid blocks employed to represent the zones at the top and bottom of the vessel, respectively. The interior of the vessel (rock loading and water in the voids) is represented by a one-dimensional column of 30 disk-shaped elements (5 per layer). This column is surrounded by two columns of concentric rings, which represent the vessel wall and the (ambient) boundary conditions, respectively. Each interior element is further sub-partitioned into a one-dimensional string of 4-8 elements, so that heat conduction from the interior of the rock blocks to the surfaces, and subsequent heat transfer to the invading cold water, can be modeled in quantitative detail. The sub-partitioning is based on the method of "multiple interacting continua", or MINC, as developed by Pruess and Narasimhan (1982). Specific details on the mesh generation methodology are described by Pruess and Karasaki (1982).

Calculations were carried out with Lawrence Berkeley Laboratory's geothermal simulators SHAFT79 and MULKOM (Pruess and Schroeder, 1980). These simulators feature an accurate representation of the thermophysical properties of water substance (International Formulation Committee, 1967). Handbook values were used for the thermal parameters of the steel vessel and the rock loading. Figure 2 shows the comparison of the simulated temperature transients with the experimental measurements for run 5-1. The overall agreement is rather good, considering that no adjustments were made in the parameters employed in the simulation. The largest discrepancies occur for the bottom layer (B-plane in Figure 2), and are probably due to too coarse discretization near the cold water inlet. Temperatures in the M-plane agree better, with the simulation predicting a somewhat too broad distribution. The best comparison is obtained near the top (T-plane).

These results are certainly encouraging, and improvements in various details of the model to obtain a better match of the experiments are in progress. These efforts focus on: (1) improving the computational mesh to more faithfully represent the physical model, and (2) checking on the thermal parameters of the system components. The simulation shows that heat transfer from the steel vessel to the injected water is of the same order of magnitude as heat transfer from the rocks. Therefore, heat conduction in the vessel walls and heat loss to the surroundings must be modeled with a high degree of accuracy. Work is in progress to adjust the heat loss term in the numerical model. It is evident from the predictions given in Figure 5 for the cooldown experiment using the present numerical model that model heat losses are greater than actual physical system heat losses. Once the heat loss term has been adjusted the calculations should be sufficiently sensitive to the rock-water heat transfer to allow quantitative testing of the approximations made in the MINC-method.

The heat extraction experiments were also modeled using the one-dimensional cold-water sweep model. The rock geometry in this model is represented by uniform size spheres with an equivalent diameter resulting in heat transfer characteristics that are similar to those of the actual rock configurations (Iregui et al. 1978).

The predicted water temperatures in the three planes are compared to measured temperatures in Figures 2 through 4 for experiments 5-1 through 5-3, respectively. The comparisons show that the predicted temperatures are generally higher than the experimental temperatures during early times but tend to drop more rapidly at later times. In contrast, the distributed numerical model predicted a cooldown which was generally slower than the experimental results during later times.

CONCLUSIONS

Three heat extraction experiments using a known-geometry rock loading and a calibration cooldown experiment for this rock loading yielded a set of useful hydrothermal reservoir production data covering a range of cooldown rates. The one-dimensional sweep model being developed for early use in hydrothermal reservoirs shows good agreement with the experimental data. A numerical model of the experimental system is under development and early predictions indicate reasonable agreement between numerical model output and experimental results. Future efforts will concentrate on improving details of the model particularly those related to experimental system heat loss characteristics. Once completed, a more detailed evaluation of the rock heat transfer process and appropriate simplified modeling approaches for use in the one-dimensional sweep model can be made.

REFERENCES

Hunsbedt, A., P. Kruger, and A. L. London, "Recovery of Energy from Fracture-Stimulated Geothermal Reservoirs," Journal of Petroleum Technology, August 1977.

Hunsbedt, A. , P. Kruger, and A. L. London, "Laboratory Studies of Fluid Production from Artificially Fractured Geothermal Reservoirs," Journal of Petroleum Technology, May 1978.

International Formulation Committee, "A Formulation of the Thermodynamic Properties of Ordinary Water Substance", IFC Secretariat, Dusseldorf, Germany, 1967.

Iregui, R., A. Hunsbedt, P. Kruger, and A. L. London, "Analysis of Heat Transfer and Energy Recovery in Fractured Geothermal Reservoirs", Stanford Geothermal Report SGP-TR-31, June 1978.

Pruess, K. and Karasaki, K., "Proximity Functions for Modeling Fluid and Heat Flow in Reservoirs with Stochastic Fracture Distributions", Proceedings, Eighth Workshop on Geothermal Reservoir Engineering, Stanford University, Stanford, December 1982.

Pruess, K. and Narasimhan, T. N., "A Practical Method for Modeling Fluid and Heat Flow in Fractured Porous Media", Proc. Sixth SPE-Symposium on Reservoir Simulation (paper SPE-10509), New Orleans, 1982.

Pruess, K. and Schroeder, R. D., SHAFT79 User's Manual, LBL-10861, Lawrence Berkeley Laboratory, Berkeley, 1980.

Swenson, Jr., L. W. and A. Hunsbedt, "Experimental and Finite Element Analysis of the Stanford Hydrothermal Reservoir Model", Proceedings, Seventh Workshop Geothermal Engineering, Stanford, December 1981.

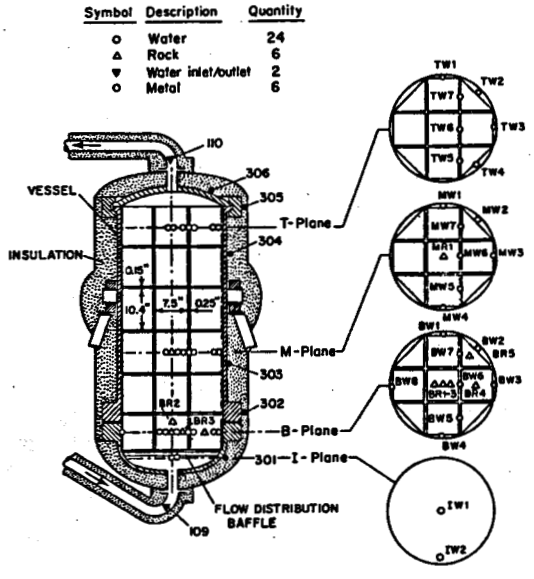

Figure 1. Experimental Rock Matrix Configuration and Thermocouple Locations.

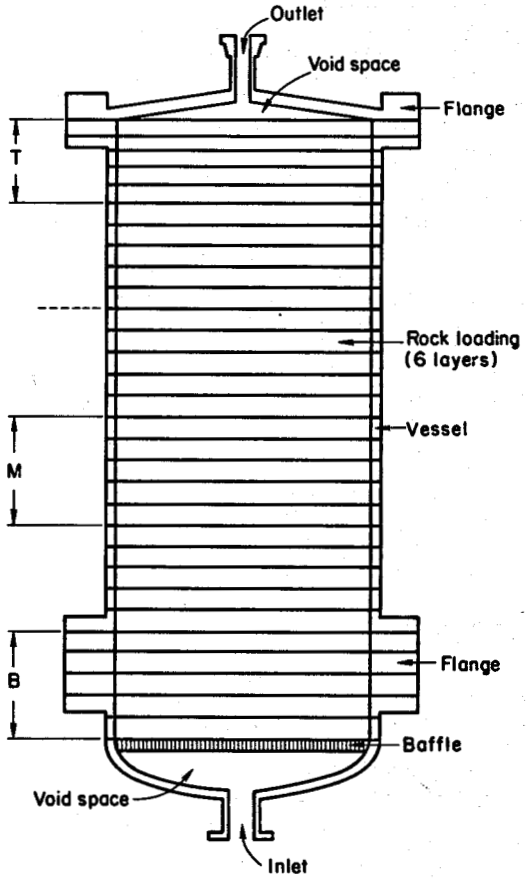

Figure 6. Basic Computational Mesh of the of Experimental System.

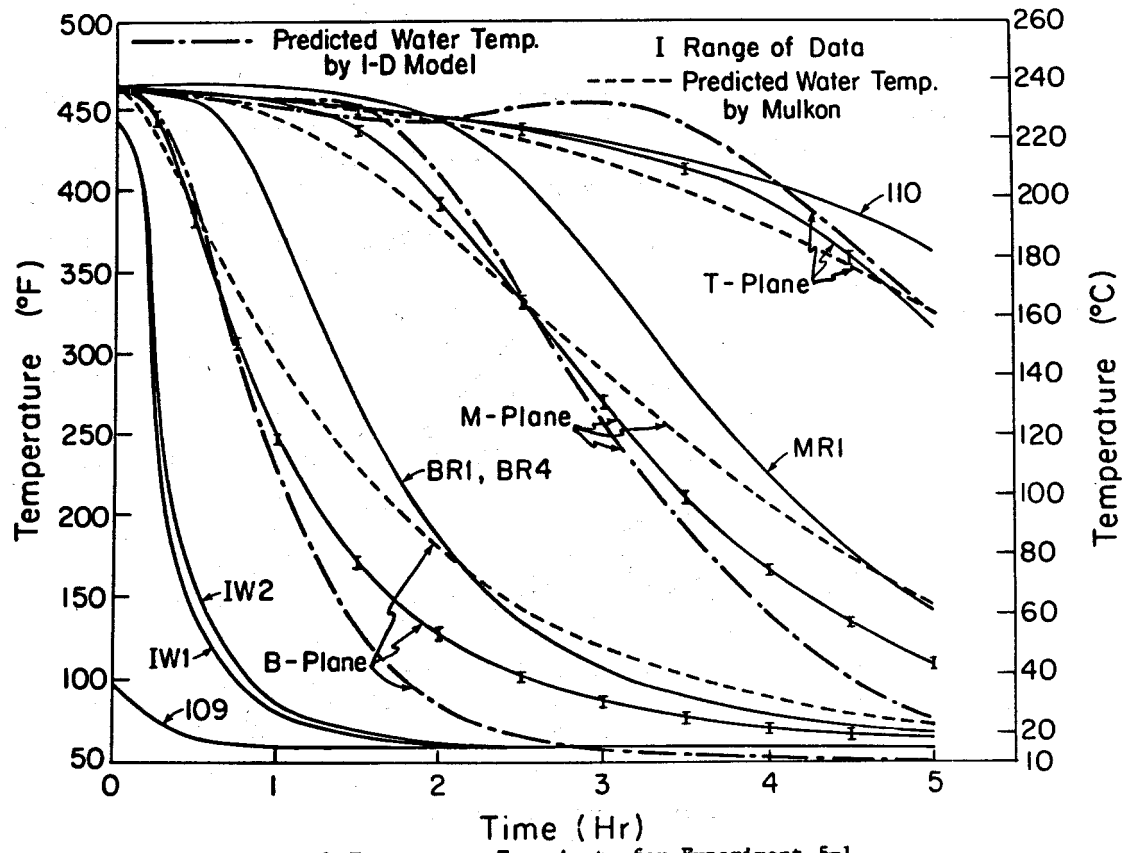

Figure 2. Water and Rock Temperature Transients for Experiment 5-1.

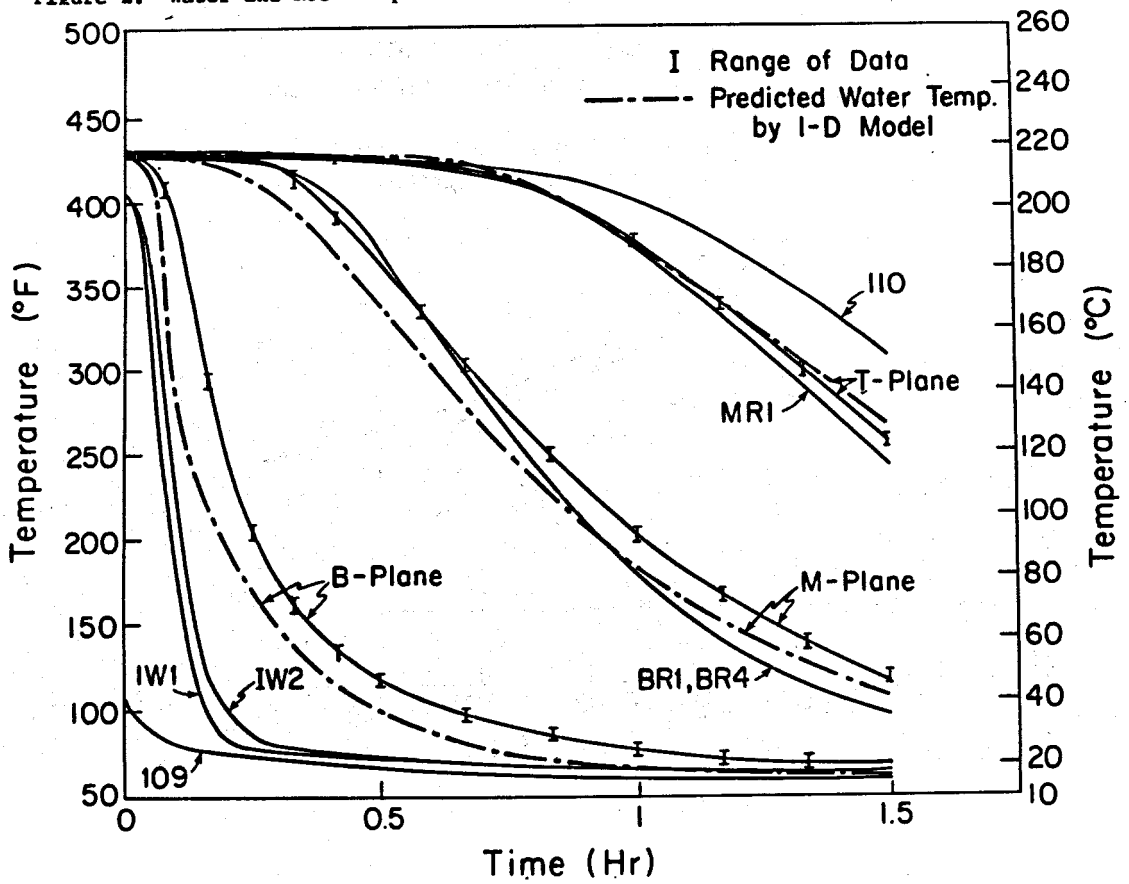

Figure 3. Water and Rock Temperature Transients for Experiment 5-2.

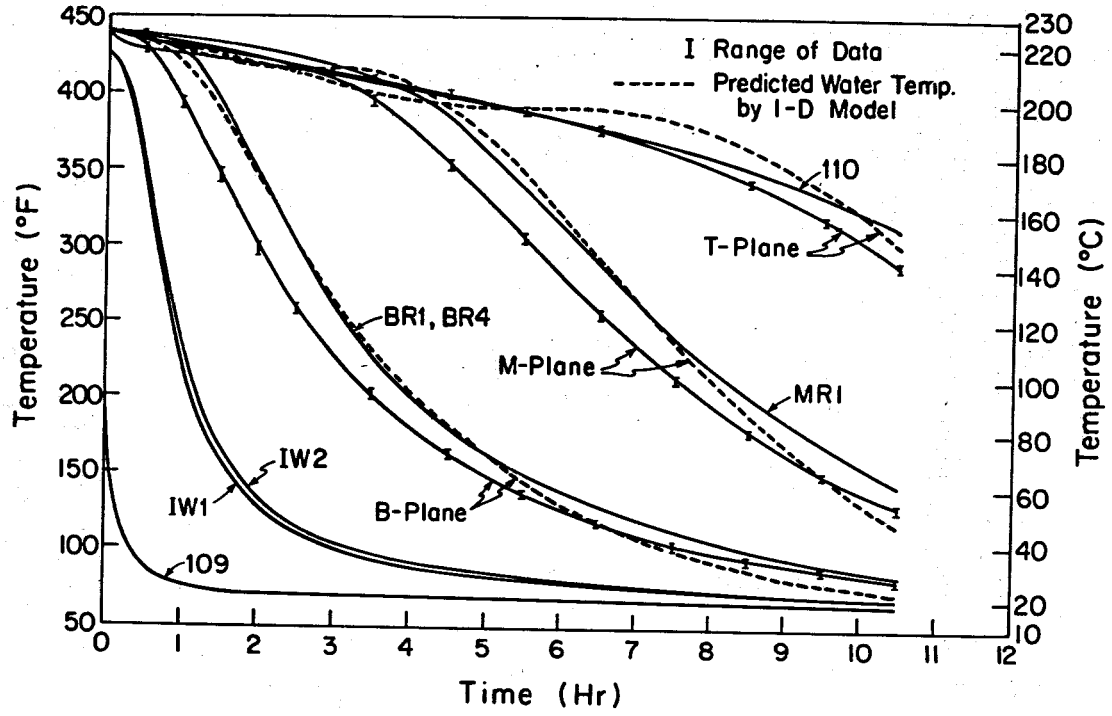

Figure 4. Water and Rock Temperature Transients for Experiment 5-3.

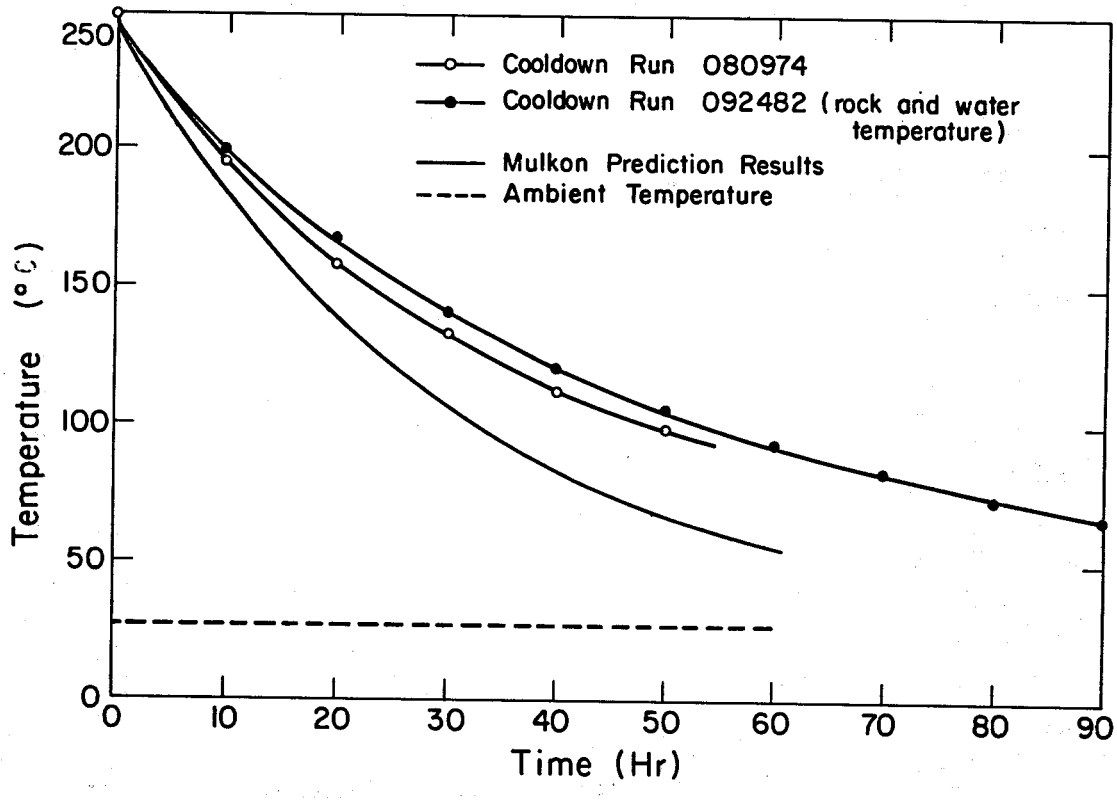

Figure 5. Average Vessel Temperature Transients for Calibration Experiment.